



Dark matter through the quark vector current portal

DILLON BERGER¹, ARVIND RAJARAMAN^{1,*} and JASON KUMAR²

¹Department of Physics and Astronomy, University of California, Irvine, CA 92697, USA

²Department of Physics and Astronomy, University of Hawai'i, Honolulu, HI 96822, USA

*Corresponding author. E-mail: arajaram@uci.edu

MS received 6 April 2020; revised 20 May 2020; accepted 18 June 2020

Abstract. We consider models of light dark matter coupled to quarks through a vector current interaction. For low energies, these models must be treated through the effective couplings to mesons, which are implemented here through the chiral Lagrangian. We find the signals of dark matter annihilation and decay to the light mesons, and find the expected photon spectrum from the decay of the hadrons. We compare the current and future observations, and show that there is a significant discovery reach for these models.

Keywords. Indirect detection; light dark matter; gamma rays; chiral Lagrangian.

PACS Nos 95.35.+d; 95.55.Cs; 11.30.Rd

1. Introduction

Recently, there has been significant interest in models of dark matter (DM) in which the DM particle has a mass $m_X \lesssim \mathcal{O}(\text{GeV})$. These models can evade the tight constraints on DM placed by direct detection experiments, as these experiments typically lose sensitivity at low mass. If DM with $m_X \lesssim \mathcal{O}(\text{GeV})$ annihilates or decays in the cosmos, the photons produced will tend to lie in the current ‘MeV-gap’ in observational sensitivity, but a variety of new instruments (such as e-ASTROGAM [1], AMEGO [2] and APT [3]) are being developed to fill this gap. Such instruments would be well-positioned for indirect detection searches for MeV-range DM.

Recently, there has been particular interest in MeV-range DM which couples largely to light quarks [4–10]. The reason is that the hadronic final states which can be produced at such small centre-of-mass energies are largely constrained by kinematics and symmetry. Moreover, several accessible hadrons, such as π^0 and η , produce striking photon signals when they decay. This scenario is thus particularly appealing from the point of view of indirect detection.

Recent work has considered the case where DM couples to either scalar, pseudoscalar, or axial-vector quark bilinears [10]. But if DM couples to a quark vector current, then the leading accessible final state (at low centre-of-mass energy) is $\pi^+\pi^-$, whose decays produce few photons, making this case difficult to probe.

In this work, we extend this analysis to higher energies, where new final states are allowed. We determine the photon spectrum which will be produced for a variety of choices of the flavour structure of DM–standard model (SM) interactions, and determine the sensitivity of the proposed experiments.

We shall be interested in the case where DM appears as a vector spurion. We assume that electroweak couplings are only relevant for the decays of hadrons produced by DM annihilation/decay. As described in [10] (see also [11]), DM–SM interactions can then be understood using chiral perturbation theory, where DM is introduced as a spurion which breaks SM flavour symmetries. The chiral Lagrangian used for the analysis in [10] only involved the pseudoscalar meson octet. But, as this work will consider a higher mass range, we must also introduce the vector meson octet, following the approach of [12]. We shall find that the dominant photon signal arises from the production of π^0 , either directly or from the decays of K_L , K_S , K^\pm , ρ or ω .

The plan of this paper is as follows. In §2, we shall describe the application of chiral perturbation theory to the interaction of low-mass DM with quark vector currents. In §3, we shall describe the generation of the photon spectrum through primary and secondary decays of the hadronic final-state particles. In §4, we shall present the sensitivities which can be expected from the proposed experiments. We conclude with a discussion of our results.

2. The application of chiral perturbation theory to dark matter interactions with vector currents

We shall consider two models in which DM either decays or annihilates through a coupling to the vector quark current. In the first model of DM decay, a single spin-1 DM particle (X_μ) couples to the vector quark current and can decay to SM particles. For this model,

$$\mathcal{L}_{\text{int}} = g \sum_q \alpha_q X^\mu \bar{q} \gamma_\mu q. \quad (1)$$

In the second model, we take DM to be a Dirac fermion (χ) which couples to quarks through a vector–vector interaction. In this model we take

$$\mathcal{L}_{\text{int}} = \sum_q \frac{\alpha_q}{\Lambda^2} \bar{\chi} \gamma^\mu \chi \bar{q} \gamma_\mu q. \quad (2)$$

For the application to chiral perturbation theory, it is useful to consider these interactions as couplings of the quark vector current to a spurion v_q^μ where

$$v_q^\mu = g \alpha_q X^\mu \quad \text{or} \quad \frac{\alpha_q}{\Lambda^2} \bar{\chi} \gamma^\mu \chi. \quad (3)$$

Note that this interaction generically breaks the $SU(3)_L \times SU(3)_R$ flavour symmetries of low-energy QCD.

We note that there is a specific case, viz. $\alpha_u = -2\alpha_d = -2\alpha_s$, which corresponds to the electromagnetic coupling. For this particular coupling, the DM annihilation rates can be obtained by using data from e^+e^- to hadrons. However, for a more general relation between the couplings, we cannot use this data, and the chiral Lagrangian is essential.

We shall take the mass of DM to be in the GeV range; we shall be more specific shortly. In this range, the decay/annihilation products cannot be treated as weakly coupled propagating quarks. We assume that the dominant final states produced by low-mass DM interactions with quarks are hadronic, and that primary interactions which scale as α_{EM} or sG_F are negligible. As the coupling of DM to light hadrons is governed by QCD and the dark matter–quark current contact interaction, we can directly express the coupling of DM to light mesons using a chiral Lagrangian in which DM appears as a spurion which breaks SM flavour symmetries.

This approach was followed in [10], under the assumption that $\sqrt{s} \lesssim 2m_{K^\pm}$. In this case, the only accessible hadrons are π^0 , π^\pm and η , and one can describe DM–SM interactions using a chiral Lagrangian involving only the spurions and the pseudoscalar meson octet. But in the case in which DM only interacted with quark vector currents, it was found that the only accessible two-body final state was $\pi^+\pi^-$. As the decays of charged pions produce very few photons, this channel

is not useful for the purpose of indirect detection with γ -ray telescopes.

We now redo this analysis for DM masses where vector mesons are kinematically accessible. We shall focus on the energy range $0.91 \text{ GeV} \leq E_{\text{cm}} \leq 1.15 \text{ GeV}$. Below this energy range, the only two-body final state which is allowed by symmetry and kinematics is $\pi^+\pi^-$, and this state produces few photons, leading to reduced sensitivity for γ -ray experiments. We also do not consider larger energies, in order to avoid final states involving glueballs.

The allowed final states from a DM initial state are restricted by symmetry considerations. The only kinematically accessible neutral two-body final states with vanishing net strangeness are $\pi\pi$, $\eta\eta$, $\eta\pi^0$, $\rho\pi$, $\omega\pi^0$, K^+K^- , $K^0\bar{K}^0$. If DM couples to a vector quark current, the final state necessarily has $J^{\text{PC}} = 1^{--}$. As such, the $\pi^0\pi^0$, $\eta\pi^0$, $\eta\eta$, $K_L K_L$ and $K_S K_S$ final states are forbidden. As a result, the only final states which we need to consider are $\pi^+\pi^-$, K^+K^- , $K^L K^S$, $\rho\pi$ and $\omega\pi^0$. We shall use the chiral Lagrangian to see that indeed all these final states can be accessed.

We write the chiral Lagrangian for the pseudoscalar meson octet to lowest order in the p^2 expansion. As the flavour symmetries of low-energy QCD are broken by the insertion of v_q^μ in the fundamental Lagrangian through eq. (1), v_q^μ must also appear in the chiral Lagrangian as spurions which break the flavour symmetries. The form of these interactions is determined at this order by symmetry considerations, and chiral Lagrangian can be expressed (see [13]) as

$$\mathcal{L}_\Phi = \frac{F^2}{4} \text{Tr}[(\partial_\mu U - i v_\mu U + i U v_\mu) \times (\partial^\mu U^\dagger + i U^\dagger v_\mu - i v_\mu U^\dagger)], \quad (4)$$

where

$$U \equiv \exp[i\sqrt{2}\Phi/F],$$

$$\Phi \equiv \begin{pmatrix} \frac{\pi^0}{\sqrt{2}} + \frac{\eta_8}{\sqrt{6}} & \pi^+ & K^+ \\ \pi^- & -\frac{\pi^0}{\sqrt{2}} + \frac{\eta_8}{\sqrt{6}} & K^0 \\ K^- & \bar{K}^0 & -\frac{2\eta_8}{\sqrt{6}} \end{pmatrix},$$

$$v^\mu \equiv \begin{pmatrix} v_u^\mu & 0 & 0 \\ 0 & v_d^\mu & 0 \\ 0 & 0 & v_s^\mu \end{pmatrix}. \quad (5)$$

The pion decay constant is $F \sim 92 \text{ MeV}$. To a good approximation, η_8 can be equated with the physical η meson, and we do so henceforth.

For the two-body final states, the only relevant terms in eq. (5) are the following contact interactions:

$$\mathcal{L}_{\text{contact}} = i\{(v_d^\mu - v_s^\mu)\bar{K}^0\partial_\mu K^0 + (v_s^\mu - v_u^\mu)K^+\partial_\mu K^- + (v_d^\mu - v_u^\mu)\pi^+\partial_\mu\pi^- - \text{h.c.}\}. \quad (6)$$

These can produce the two-body final states K^+K^- , K^L , K^S and $\pi^+\pi^-$.

Other possible two-body final states involving vector mesons may also be produced. In order to consider these final states, it is necessary to include vector mesons in the chiral Lagrangian. For this purpose, we use the results of [12]. We found that no new two-body final states can be produced directly by the contact interaction involving the vector meson octet, but they can be produced through a coupling of DM to an intermediate vector meson. We thus need the couplings of a vector meson to a vector spurion, and the trilinear couplings involving at least one vector meson. The relevant part of the chiral Lagrangian was found in [12,14], and can be written as

$$\begin{aligned} \mathcal{L}_{\Phi_{\mu\nu}} = & -\frac{1}{4}\text{Tr}[(D^\mu\Phi_{\mu\alpha})(D_\nu\Phi^{\nu\alpha})] \\ & +\frac{1}{8}m_V^2\text{Tr}[\Phi^{\mu\nu}\Phi_{\mu\nu}] \\ & +\frac{1}{2}f_V\text{Tr}[\Phi^{\mu\nu}f_{\mu\nu}^+] +\frac{i}{2}f_V h_P\text{tr}(U_\mu\Phi^{\mu\nu}U_\nu) \\ & +\frac{i}{8}h_A\varepsilon^{\mu\nu\alpha\beta}\text{tr}(\{\Phi_{\mu\nu}, (D^\tau\Phi_{\tau\alpha})\}U_\beta) \\ & +\frac{i}{8}h_O\varepsilon^{\mu\nu\alpha\beta}\text{tr}([D_\alpha\Phi_{\mu\nu}, \Phi_{\tau\beta}]U^\tau), \end{aligned} \quad (7)$$

where

$$\Phi_{\mu\nu} = \sqrt{2} \begin{pmatrix} \frac{\rho_{\mu\nu}}{\sqrt{2}} + \frac{\omega_{\mu\nu}}{\sqrt{2}} & \rho_{\mu\nu}^+ & K_{\mu\nu}^{*+} \\ \rho_{\mu\nu}^- & -\frac{\rho_{\mu\nu}}{\sqrt{2}} + \frac{\omega_{\mu\nu}}{\sqrt{2}} & K_{\mu\nu}^{*0} \\ K_{\mu\nu}^{*-} & \bar{K}_{\mu\nu}^{*0} & \phi_{\mu\nu} \end{pmatrix},$$

$$f_{\mu\nu}^+ = \frac{1}{2}[e^{i\Phi/\sqrt{2}F}(\partial_\mu v_\nu - \partial_\nu v_\mu)e^{-i\Phi/\sqrt{2}F} + e^{-i\Phi/\sqrt{2}F}(\partial_\mu v_\nu - \partial_\nu v_\mu)e^{i\Phi/\sqrt{2}F}],$$

$$U_\mu = \frac{1}{2}e^{-i\Phi/\sqrt{2}F}(\partial_\mu e^{i\sqrt{2}\Phi/F})e^{-i\Phi/\sqrt{2}F} - \frac{i}{2}e^{-i\Phi/\sqrt{2}F}v_\mu e^{i\Phi/\sqrt{2}F} + \frac{i}{2}e^{i\Phi/\sqrt{2}F}v_\mu e^{-i\Phi/\sqrt{2}F},$$

$$D_\alpha\Phi_{\mu\nu} = \partial_\alpha\Phi_{\mu\nu} + [\Gamma_\alpha, \Phi_{\mu\nu}],$$

$$\Gamma_\alpha = \frac{1}{2}e^{-i\Phi/\sqrt{2}F}(\partial_\mu - i v_\mu)e^{i\Phi/\sqrt{2}F} + \frac{1}{2}e^{i\Phi/\sqrt{2}F}(\partial_\mu - i v_\mu)e^{-i\Phi/\sqrt{2}F}.$$

The cubic couplings between the vector and pseudoscalar meson octets are

$$\begin{aligned} \mathcal{L}_{\text{int}} \supset & -\frac{\sqrt{2}h_A}{F}\varepsilon^{\mu\nu\alpha\beta}\left[\frac{1}{2}\partial_\beta\pi^0(\rho_{\mu\nu}^0\partial^\tau\omega_{\tau\alpha} + \omega_{\mu\nu}\partial^\tau\rho_{\tau\alpha}^0) \right. \\ & \left. +\partial_\beta\pi^-(\rho_{\mu\nu}^+\partial^\tau\omega_{\tau\alpha} + \omega_{\mu\nu}\partial^\tau\rho_{\tau\alpha}^+) + \text{c.c.}\right] \\ & -\frac{h_O}{\sqrt{2}F}\varepsilon^{\mu\nu\alpha\beta}[(\partial_\alpha\rho_{\mu\nu}^0)((\partial^\tau\pi^0)\omega_{\tau\beta}) \\ & +\rho_{\tau\beta}^0((\partial^\tau\pi^0)\partial_\alpha\omega_{\mu\nu}) + (\partial^\tau\pi^-(\omega_{\tau\beta}\partial_\alpha\rho_{\mu\nu}^+ \\ & +\rho_{\tau\beta}^+\partial_\alpha\omega_{\mu\nu}) + \text{c.c.})] \\ & +i\frac{8f_V h_P}{F^2}[2\partial_\mu\pi^+\partial_\nu\pi^-\rho_{\mu\nu}^0 \\ & +\partial_\mu\bar{K}^0\partial_\nu K^0(\rho_{\mu\nu}^0 - \omega_{\mu\nu} - \sqrt{2}\varphi_{\mu\nu}) \\ & -\partial_\mu K^-\partial_\nu K^+(\rho_{\mu\nu}^0 + \omega_{\mu\nu} - \sqrt{2}\varphi_{\mu\nu})], \end{aligned} \quad (8)$$

where m_V , f_V , h_A , h_O and h_P are parameters (the values of the relevant parameters are given in §5.1).

From these interactions, we find two new possible final states: $\rho\pi^0$ and $\omega\pi^0$.

3. Photon spectra

These primary mesons can then decay through multiple decay modes to produce photons. These can be multi-step decay processes; for example, the kaon can decay to pions which subsequently decay to photons. In our case, the primary mesons are π^0 , π^\pm , K^0 , \bar{K}^0 , K^\pm , ρ , ω , and we need to find the photon spectra produced in their decays. The π^0 decays to two photons essentially 100% of the time, and the π^\pm essentially never produce photons. The ρ^0 decays primarily to charged pions, and hence does not produce photons. But decays of ρ^\pm typically produce π^0 as well as π^\pm , with the subsequent decays of π^0 yielding photons. For the kaons and the omega, we use the decay modes found in the Particle Data Book [15]. We have tabulated in table 1 the important decay modes of the mesons which we have considered, along with their branching ratios. Decay modes which are not expected to produce a significant number of photons (e.g. decays involving only charged pions) are not shown.

For the two-body decays, the decay spectrum at rest is fixed by kinematics. The three-body decays are described by a Dalitz plot, which parametrises the decay kinematics in terms of the final-state energies. We use these to find the decay spectrum at rest for each decay mode of each meson. These details are presented in Appendix A. Finally, these mesons are produced and decay with large boosts which also modify the spectrum.

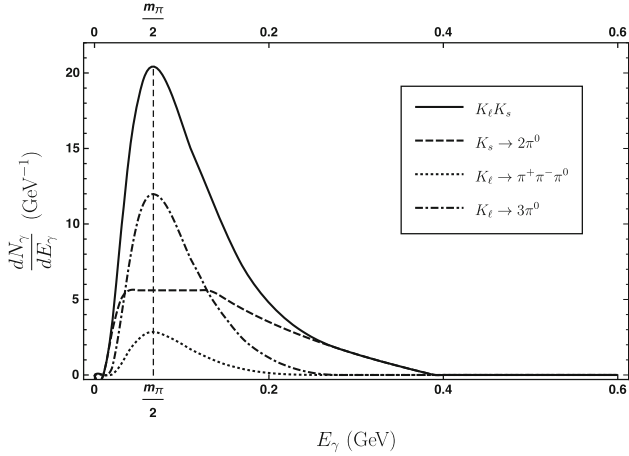


Figure 1. Photon spectrum from neutral kaon production ($K_L K_S$). The centre-of-mass energy has been taken to be 1.14 GeV.

The boosting procedure is general, and is described in Appendix B.

For illustrative purposes, we show in figure 1 the photon spectrum obtained through the production of neutral kaons produced from DM is annihilation or decay, assuming $E_{\text{cm}} = 1.14$ GeV. The individual spectrum has been weighted according to the branching fractions. It is interesting to compare this spectrum to those found in [10], for the case where DM is coupled to scalar, pseudoscalar or axial-vector quark currents. In those cases, even though the centre-of-mass energy was taken to be ≤ 1 GeV, the typical photon energy was nearly four times larger than that found here, because in the case of a scalar, pseudoscalar or axial-vector spurion, one can produce an η in the final state, whose decay yields photons and in the case of a vector spurion, however, almost all photons arise from π^0 decay. As is discussed in Appendix B, the photons produced by π^0 decay yield a signal with a peak at $m_\pi/2$, as can be seen in figure 1, resulting in a typical photon energy which is considerably smaller than that of the photons produced from η decay.

Table 1. The relevant decay modes and branching fractions for the mesons produced from DM annihilation/decay through the quark vector current portal.

K^+	$\pi^0 e^+ \nu$	5%	K^S	$\pi^0 \pi^0$	30.7%	
	$\pi^0 \mu^+ \nu$	3.4%		K^L	$\pi^0 \pi^0 \pi^0$	19.5%
	$\pi^+ \pi^0$	20.7%			$\pi^+ \pi^- \pi^0$	12.5%
	$\pi^+ \pi^0 \pi^0$	1.7%		ω	$\pi^+ \pi^- \pi^0$	89%
ρ^\pm	$\pi^\pm \pi^0$	100%		$\pi^0 \gamma$	8%	

Table 2. Average number of photons produced within the energy window from a single DM decay/annihilation process, given that the particles in the left-most column are produced.

Channel	N_p
$K^+ K^-$	0.2471
$K_L K_S$	0.7599
$\rho^0 \pi^0$	0.31473
$\omega^0 \pi^0$	0.72438
$\rho^\pm \pi^\mp$	0.24213

4. Comparisons to observations

Following [10], we consider constraints on the obtained photon spectrum from observations of diffuse photon emission, and from future observations of photon emission from a dwarf galaxy (Draco). We shall take as a benchmark, an experiment with a fractional 1σ energy resolution of $\epsilon = 0.3$ and an exposure of $I_{\text{exp}} = 3000 \text{ cm}^2 \text{ yr}$. As our predicted signal peak is at $m_\pi/2$, we shall consider a bin of photon energies centred at $E_0 = m_\pi/2$ and a width of $0.3E_0$, i.e. a bin between $E_- = (m_\pi/2)(1 - \epsilon)$ and $E_+ = (m_\pi/2)(1 + \epsilon)$. We account for instrumental energy resolution by convolving the injected photon spectrum with a Gaussian smearing function

$$R_\epsilon(E_{\text{obs.}}, E_\gamma) = \frac{1}{\sqrt{2\pi}\epsilon E_\gamma} \exp\left(-\frac{(E_{\text{obs.}} - E_\gamma)^2}{2\epsilon^2 E_\gamma^2}\right). \quad (9)$$

For each channel p , we determine how many photons are produced per annihilation/decay within the energy bin $E_- \leq E \leq E_+$. These are listed as N_p in table 2.

For the annihilation process, we define an effective cross-section $\langle\sigma v\rangle_{\text{eff}}$ by weighting the theoretical cross-sections for each channel p with the acceptance factor N_p , and similarly we define the effective decay lifetime Γ_{eff} ; explicitly

$$\langle\sigma v\rangle_{\text{eff}} = \sum_{\text{channels}} \langle\sigma v\rangle_p N_p = \langle\sigma v\rangle_{\text{total}} \langle N_p \rangle$$

$$\Gamma_{\text{eff}} = \sum_{\text{channels}} \Gamma_p N_p = \Gamma_{\text{total}} \langle N_p \rangle, \quad (10)$$

where

$$\langle N_p \rangle \equiv \sum_{\text{channels}} Br_p N_p, \quad (11)$$

and where $\langle\sigma v\rangle_{\text{total}}$ is the total annihilation cross-section, Γ_{total} is the total decay width and Br_p is the branching fraction to channel p .

Given the branching fractions to all final states, one can compute $\langle N_p \rangle$, and a bound obtained from data on

$\langle\sigma v\rangle_{\text{eff}}$ or Γ_{eff} can be directly translated into a bound on the total annihilation cross-section or decay width.

Note that, for all the channels given in table 2, the highest and lowest N_p differ by at most a factor of 3. Although the branching fractions could be computed using the chiral Lagrangian, one could worry about higher-order corrections. However, as long as DM annihilation/decay proceeds almost entirely to the final states that we consider (i.e. if $\sum_{\text{channels}} Br_p \sim 1$), then $\langle N_p \rangle$ can be corrected by at most a factor of ~ 3 , as that is the largest ratio of acceptance factors between any channels. Thus, these corrections could only change bounds on the total annihilation cross-section or decay rate by a factor of at most ~ 3 . The only exception is the $\pi^+\pi^-$ final state, for which $N_p \sim 0$; if this final state is allowed by the symmetries of the theory, then the relationship between the effective annihilation cross-section (decay width) and the total annihilation cross-section (decay width) is more dependent on the branching fractions. But this final state is not allowed if $\alpha_u = \alpha_d$, as a result of isospin symmetry. Moreover, the branching fraction to $\pi^+\pi^-$ is related to the branching fraction to K^+K^- and $K_L K_S$ by flavour symmetry, as seen from eq. (6). As such, the ratio of these branching fractions cannot receive large corrections.

The total photon signal N_S is

$$N_S = \frac{\Xi_{\text{eff}}^{\text{ann.,dec.}}}{4\pi m_X} \bar{J}^{\text{ann.,dec.}} (I_{\text{exp}} \Delta\Omega), \quad (12)$$

where

$$\Xi^{\text{ann.}} = \frac{\langle\sigma_A v\rangle_{\text{eff}}}{2m_X}, \quad \Xi^{\text{dec.}} = \Gamma_{\text{eff}} \quad (13)$$

and $\bar{J}^{\text{ann.,dec.}}$ are the average J -factors of the target for either DM annihilation or DM decay. For diffuse emission, the average J -factors are [16]

$$\begin{aligned} \bar{J}_{\text{dif.}}^{\text{ann.}} &= 3.5 \times 10^{21} \text{ GeV}^2 \text{ cm}^{-5} \text{ sr}^{-1}, \\ \bar{J}_{\text{dif.}}^{\text{dec.}} &= 1.5 \times 10^{22} \text{ GeV cm}^{-2} \text{ sr}^{-1}, \end{aligned} \quad (14)$$

while for Draco, the average J -factors are [17]

$$\begin{aligned} \bar{J}_{\text{Draco}}^{\text{ann.}} &= 6.94 \times 10^{21} \text{ GeV}^2 \text{ cm}^{-5} \text{ sr}^{-1}, \\ \bar{J}_{\text{Draco}}^{\text{dec.}} &= 5.77 \times 10^{21} \text{ GeV cm}^{-2} \text{ sr}^{-1}. \end{aligned} \quad (15)$$

5. Results

For diffuse emission, we restrict attention to latitudes greater than $>20^\circ$. In this region, and in the energy range 0.8 MeV–1 GeV, the isotropic flux observed by COMPTEL and EGRET can fit well with [4,18] the function

$$\frac{d^2\Phi^{\text{iso.}}}{d\Omega dE_{\text{obs.}}}$$

$$= 2.74 \times 10^{-3} \left(\frac{E_{\text{obs.}}}{\text{MeV}} \right)^{-2.0} \text{ cm}^{-2} \text{ s}^{-1} \text{ sr}^{-1} \text{ MeV}^{-1}. \quad (16)$$

The expected number of observed events between the energies E_- and E_+ is then given by

$$N_O = 8.6 \times 10^4 \left(\frac{\text{MeV}}{E_-} - \frac{\text{MeV}}{E_+} \right) \frac{(I_{\text{exp.}} \Delta\Omega)}{\text{cm}^2 \text{ yr sr}}. \quad (17)$$

We impose the condition that within any such energy bin, the number of expected signal events should not exceed the number of expected observed events, i.e., we require $N_S < N_O$. This constitutes a conservative bound; since we assume no knowledge of the background photon spectrum, we conservatively assume that the background could be negligible in any energy bin.

For a dwarf spheroidal galaxy, such as Draco, the background consists of all photons emitted by astrophysical processes as well as DM annihilation/decay along the line of sight to the dwarf, but not within the dwarf. This background can be estimated purely from the data by considering the observed flux in the direction of the dSph, but slightly off-axis [17–21]. Although one would follow this approach in the actual analysis of data from a future instrument, for our purposes, we can estimate the background flux to be roughly equal to the observed diffuse flux given in eq. (16). If we assume that the number of observed events is the same as the expected number of background events, then a model can be ruled out at $n - \sigma$ confidence level if $N_S > n\sqrt{N_O}$. We also assume that the experimental angular resolution is smaller than the size of Draco (1.3°).

The constraint on DM annihilation from the diffuse emission is

$$\langle\sigma_A v\rangle_{\text{eff}} \sim 6.22 \times 10^{-26} \text{ cm}^3 \text{ s}^{-1} \quad (18)$$

while the constraint on the lifetime is

$$\Gamma_{\text{eff}} \sim 2.55 \times 10^{-26} \text{ s}^{-1}. \quad (19)$$

A similar study of DM annihilation/decay in Draco could yield a 2σ constraint on DM annihilation of

$$\langle\sigma_A v\rangle_{\text{eff}} \lesssim 9.83 \times 10^{-28} \text{ cm}^3 \text{ s}^{-1} \quad (20)$$

while the constraint on the lifetime would be

$$\Gamma_{\text{eff}} \lesssim 2.07 \times 10^{-27} \text{ s}^{-1}. \quad (21)$$

The Planck bound on the rate of electromagnetic decays is $\Gamma_{\text{total}} \sim \mathcal{O}(10^{-24}) \text{ s}^{-1}$ [4,24,25]. Our sensitivity is to the effective decay width, which differs from Γ_{total} by a factor $\langle N_p \rangle$ (which depends on the flavour structure of the quark couplings). But this factor is always $\mathcal{O}(1)$ for any choice of flavour structure, and so the sensitivity obtainable from indirect detection is

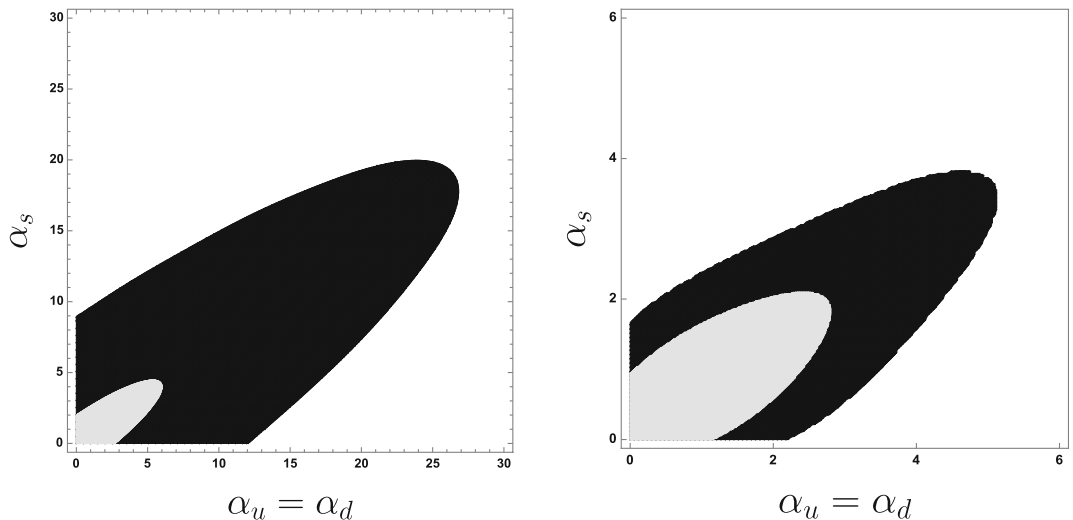


Figure 2. Bounds on the parameter space from annihilation (left panel, $\Lambda = 100$ GeV) and decay (right panel, $g = 10^{-24}$) on theories with $\alpha_u = \alpha_d$, assuming $E_{cm} = 1.14$ GeV. The region in black is allowed by constraints on diffuse emission, while the grey region demarcates the sensitivity of a search for emission from Draco.

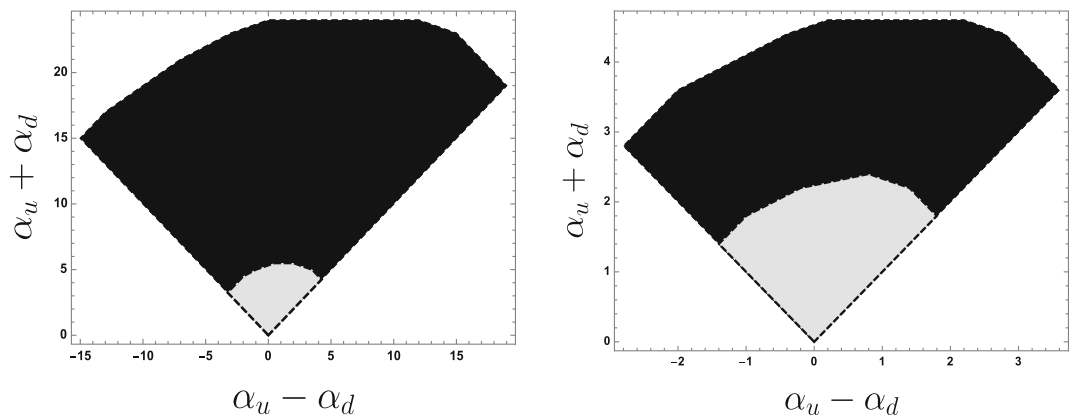


Figure 3. Bounds on the parameter space from annihilation (left panel, $\Lambda = 100$ GeV) and decay (right panel, $g = 10^{-24}$) on theories with $\alpha_s = 0$, assuming $E_{cm} = 1.14$ GeV. The region in black is allowed by constraints on diffuse emission, while the grey region demarcates the sensitivity of a search for emission from Draco.

typically at least an order of magnitude better than the Planck bound.

We can also convert these to bounds on the fundamental couplings. This calculation is contaminated by uncertainties in the chiral Lagrangian at high energies. Nevertheless, we now present estimates for such bounds in §5.1.

5.1 Tree-level bounds on parameters

Here we calculate the bounds on the fundamental scale corresponding to the bounds on the effective cross-section and lifetime found earlier. We work to tree level in the chiral Lagrangian; higher-order effects may produce deviations from these results, but we believe that our estimates should be accurate to a factor of order 1.

We calculate the cross-section using the Lagrangians (eqs (5), (7), (8)). The various parameters are [12,14]

$$\begin{aligned}
 f_V &= (140 \pm 14) \text{ MeV}, \\
 m_V &\sim 0.764 \text{ GeV}, \\
 h_A &= 2.33 \pm 0.03, \\
 h_P &\sim 1.75
 \end{aligned}
 \tag{22}$$

We consider two classes of models. In the first class we assume isospin is a good symmetry, and we set $\alpha_u = \alpha_d$. In the second class we set $\alpha_s = 0$.

Bounds on the parameter space of the first class of models are shown in figure 2. Bounds on the parameter space of the second class of models are shown in figure 3. In each case, we have normalised the couplings to have $g = 10^{-24}$ in eq. (1), and $\Lambda = 100$ GeV in eq. (2). In

all cases, we have set the centre-of-mass energy to be $E_{\text{cm}} = 1.14$ GeV. Because we consider a narrow energy range lying between the $\rho\pi$ threshold (~ 0.91 GeV) and our upper cutoff (1.15 GeV), these constraints do not change dramatically as we change the centre-of-mass energy. But there is one feature worthy of note; if $E_{\text{cm}} \sim 1.02$ GeV and if DM couples to a strange quark vector current, then DM can annihilate through an intermediate ϕ near resonance. In this case, the constraints on α_s which could be obtained from indirect detection would improve dramatically. Except for energies very close to this resonance, sensitivity throughout the energy range $0.91 \text{ GeV} \leq E_{\text{cm}} \leq 1.15 \text{ GeV}$ is well approximated by results at $E_{\text{cm}} = 1.14$ GeV. Note that the ρ^0 and ω resonances lie below the kinematic range we consider.

Note also that, if the DM coupling does not break isospin, then the constraints on the couplings are weakest if $\alpha_u = \alpha_d = \alpha_s$. This can easily be understood from eq. (6); if all light quark couplings are identical, the DM coupling to the pseudoscalar meson octet vanishes. In this limit, the only remaining channels which produce photons are $\omega\pi^0$ and $\rho\pi$.

6. Conclusions

We have considered DM coupled to SM quarks through vector currents of the form $\bar{q}\gamma^\mu q$. We have utilised the chiral Lagrangian to obtain couplings of the DM to mesons, and found the photon spectrum from DM decay (if DM itself is a vector) or from annihilation (where it is a Dirac fermion). We have found that current observations of the diffuse photon spectrum already can be used to constrain the parameter space of these models. Future observations of dwarf spheroidal galaxies will significantly improve these bounds or may discover these models.

In the case of DM decay, these constraints exceed those obtainable from Planck [25] (from the effect of late-time energy injection on the CMB) by about an order of magnitude. We note that the low value of the mass weakens direct detection bounds, and for certain couplings (e.g. couplings only to strange quarks), the bounds are extremely weak. In particular, for $m_\chi \sim 500$ MeV, the upper bound on spin-independent (SI) DM–nucleon scattering found by CRESST [26] is $\sigma_{\text{SI}} \sim \mathcal{O}(10^{-1})$ pb. For a scenario of DM annihilation through coupling to the quark vector portal, DM–nucleon scattering would be spin- and velocity-independent. If we set $\alpha_u = \alpha_d \sim 3$, $\alpha_s = 0$ (the limit of sensitivity for a search for emission from Draco), one would find $\sigma_{\text{SI}} \sim \mathcal{O}(10)$ pb, which is about two orders of magnitude above the current bounds from CRESST. However, CRESST’s sensitivity is greatly reduced for the case

of isospin-violating DM [27–29] ($\alpha_u = -\alpha_d$, $\alpha_s = 0$), and is essentially unconstraining for the parameter space of interest here. Similarly, if DM only couples to the strange quark vector current ($\alpha_u = \alpha_d = 0$), then the SI scattering cross-section vanishes, and there are no meaningful constraints from direct detection.

There are several ways to extend this analysis. Consideration of 4-meson final states, and higher-order terms in the chiral Lagrangian momentum expansion, would yield subleading corrections to the photon spectrum which may nevertheless be significant, especially below the $\rho\pi$ threshold. Similarly, it may be interesting to include further particles such as glueballs.

We have found that if DM couples to a vector quark current, then the typical photon energy is roughly a factor of 4 smaller than in the scenarios considered in [10], wherein DM was coupled to scalar, pseudoscalar or axial-vector currents. This result is largely independent of the centre-of-mass energy of the process, but is instead dictated by the Lorentz and flavour structure of the DM–quark current coupling, which determines whether or not an η can be produced in the final state. It would be interesting to study more quantitatively the ability of future experiments to definitively determine the Lorentz and flavour structure of the DM–quark coupling from the photon distribution.

We hope to return to these issues in a future work.

Acknowledgements

The authors are grateful to James H Buckley, Regina Caputo and Xerxes Tata for useful discussions. JK is supported in part by DOE grant DE-SC0010504. AR is supported in part by NSF Grant PHY-1620638.

Appendix A. Decay spectra at rest

We begin by finding the decay spectrum at rest for the various mesons. For two-body decays the spectra are set by kinematics. For a decay $A \rightarrow B + C$ the energy spectrum of B is

$$\frac{d\Gamma}{dE_B} = \delta \left(E_B - \frac{m_B^2 + m_A^2 - m_C^2}{2m_A} \right). \quad (\text{A.1})$$

Three-body decays must be analysed in terms of Dalitz plots, which encode the amplitudes as a function of the kinematic variables.

Appendix A.1. $K^+(p_K) \rightarrow \bar{\ell}(p_1)\nu(p_2)\pi^0(p_3)$

The decay to $K^+(p_K) \rightarrow \bar{\ell}(p_1)\nu(p_2)\pi^0(p_3)$ is controlled by the matrix element $\mathcal{M} = (p_K + p_3)^\mu \bar{\ell}\gamma_\mu(1 -$

γ_5) v . The pion energy spectrum is controlled by

$$\Gamma = \int dm_{12}^2 dm_{23}^2 \sum_{\text{spins}} |\mathcal{M}|^2. \quad (\text{A.2})$$

We then find that

$$\begin{aligned} \frac{d\Gamma}{dm_{12}^2} \propto \int dm_{23}^2 |\mathcal{M}|^2 \propto & -8m_\ell^2(m_\pi^2 + m_\ell^2 - m_{12}^2) \\ & -8m_K^2 m_\pi^2 ((m_{23}^2)_{\text{max}} - (m_{23}^2)_{\text{min}}) \\ & +4(m_K^2 + 2m_\ell^2 + m_\pi^2 - m_{12}^2)((m_{23}^4)_{\text{max}} \\ & - (m_{23}^4)_{\text{min}}) - \frac{8}{3}((m_{23}^6)_{\text{max}} - (m_{23}^6)_{\text{min}}), \end{aligned} \quad (\text{A.3})$$

where we have defined

$$\begin{aligned} E_2^* &= \frac{m_{12}^2 - m_1^2 + m_2^2}{2m_{12}}, & E_3^* &= \frac{M^2 - m_{12}^2 - m_3^2}{2m_{12}}, \\ m_{ij}^2 &= (p_i - p_j)^2, \end{aligned}$$

$$\begin{aligned} &= 1 + g \frac{(s_3 - s_0)}{m_+^2} + h \left(\frac{(s_3 - s_0)}{m_+^2} \right)^2 \\ &+ k \left(\frac{2s_2 + s_3 - 3s_0}{m_+^2} \right)^2, \end{aligned} \quad (\text{A.5})$$

where

$$\begin{aligned} s_i &= (p_K - p_i)^2, & s_0 &= \frac{s_1 + s_2 + s_3}{3} \\ &= \frac{1}{3}(m_K^2 + m_1^2 + m_2^2 + m_3^2), \\ g &= 0.626, & h &= 0.052, & k &= 0.0054. \end{aligned} \quad (\text{A.6})$$

The pion energy distribution is then

$$\frac{d\Gamma}{dE_2} = -2m_K \frac{d\Gamma}{ds_2} \propto \int ds_3 |\mathcal{A}|^2. \quad (\text{A.7})$$

We then find that the energy distribution of π_0 in decays of $K^+ \rightarrow \pi^0 \pi^0 \pi^+$ at rest is (here E_2 is the neutral pion energy)

$$\begin{aligned} \frac{d\Gamma}{dE_2} &= \mathcal{N}_{K^+ \rightarrow \pi^+ \pi^0 \pi^0} \sigma(s_2) \\ &= \left(\alpha_0 + \alpha s_2 + \frac{\alpha_1}{s_2} + \frac{\alpha_2}{s_2^2} + \frac{\alpha_3}{s_2^3} \right), \end{aligned} \quad (\text{A.8})$$

where

$$\sigma(s_2) = \frac{\sqrt{[-2m_+^2(m_\pi^2 + s_2) + (m_\pi^2 - s_2)^2 + m_+^4][-2m_\pi^2(m_{K^+}^2 + s_2) + (m_{K^+}^2 - s_2)^2 + m_\pi^4]}}{2m_+^2} \quad (\text{A.9})$$

$$\begin{aligned} (m_{23}^2)_{\text{max}} &= (E_2^* + E_3^*)^2 - (\sqrt{(E_2^*)^2 - m_2^2} \\ &\quad - \sqrt{(E_3^*)^2 - m_3^2})^2, \\ (m_{23}^2)_{\text{min}} &= (E_2^* + E_3^*)^2 - (\sqrt{(E_2^*)^2 - m_2^2} \\ &\quad + \sqrt{(E_3^*)^2 - m_3^2})^2. \end{aligned} \quad (\text{A.4})$$

Appendix A.2. $K^+(p_K) \rightarrow \pi^0(p_1)\pi^0(p_2)\pi^+(p_3)$

The decay $K^+(p_K) \rightarrow \pi^0(p_1)\pi^0(p_2)\pi^+(p_3)$ can be expressed in terms of the invariant amplitude \mathcal{A} [15]

$$\begin{aligned} |\mathcal{A}|^2 &= \frac{d\Gamma}{ds_3 ds_2} \propto 1 + g \frac{(s_3 - s_0)}{m_+^2} + h \left(\frac{(s_3 - s_0)}{m_+^2} \right)^2 \\ &+ k \left(\frac{s_2 - s_1}{m_+^2} \right)^2 \end{aligned}$$

and

$$\left\{ \begin{aligned} \alpha_0 &= -g - \frac{2}{3}h \left(1 + \frac{m_{K^+}^2 + 2m_\pi^2}{m_+^2} \right), \\ \alpha &= \frac{2}{3m_+^2}h, \\ \alpha_1 &= 2m_+^2 + \frac{g}{3}(m_{K^+}^2 + m_+^2 + 2m_\pi^2) + \frac{h}{9} \\ &\quad \times \left(\frac{20m_\pi^4 + 2m_{K^+}^4 - 4m_\pi^2 m_{K^+}^2}{m_+^2} \right. \\ &\quad \left. + 16m_{K^+}^2 - 4m_\pi^2 + 2m_+^2 \right), \\ \alpha_2 &= g(m_\pi^2 m_{K^+}^2 - m_+^2 m_{K^+}^2 - m_\pi^4 + m_+^2 m_\pi^2) + \frac{2}{3}h \\ &\quad \times \left(\frac{m_\pi^4 m_{K^+}^2 - 2m_\pi^6}{m_+^2} + 2m_\pi^2 m_{K^+}^2 \right. \\ &\quad \left. - m_+^2 m_{K^+}^2 - m_{K^+}^4 + m_\pi^4 \right), \\ \alpha_3 &= 2h \frac{(m_+^2 - m_\pi^2)^2 (m_\pi^2 - m_{K^+}^2)^2}{3m_+^2}. \end{aligned} \right. \quad (\text{A.10})$$

We find that the normalisation constant by integrating both sides with respect to dE (picking up a factor of $-1/2m_{K^+}$). The normalisation constant is given by

$$\mathcal{N}_{K^+ \rightarrow \pi^+ \pi^0 \pi^0} = -0.00187217 \text{ (GeV)}^3.$$

Appendix A.3. $K_L(p_K) \rightarrow \pi^+(p_1)\pi^-(p_2)\pi^0(p_3), \pi^0(p_1)\pi^0(p_2)\pi^0(p_3)$

The decay $K_L(p_K) \rightarrow \pi^+(p_1)\pi^-(p_2)\pi^0(p_3)$ can be expressed in terms of the invariant amplitude \mathcal{A} [15]

$$\begin{aligned} & |\mathcal{A}(s_1, s_2, s_3)|^2 \\ &= 1 + g \frac{(s_3 - s_0)}{m_{\pi^+}^2} + h \left(\frac{s_3 - s_0}{m_{\pi^+}^2} \right)^2 \\ &+ j \frac{(s_2 - s_1)}{m_{\pi^+}^2} + k \left(\frac{s_2 - s_1}{m_{\pi^+}^2} \right)^2 \\ &+ f \frac{(s_2 - s_1)(s_3 - s_0)}{m_{\pi^+}^2} + \dots \end{aligned} \tag{A.11}$$

Here

$$\begin{aligned} s_i &= (p_K - p_i)^2, \\ s_0 &= \frac{s_1 + s_2 + s_3}{3} = \frac{1}{3}(m_K^2 + m_1^2 + m_2^2 + m_3^2), \\ g &= 0.678, \quad h = 0.076, \quad j = 0.001, \\ f &= 0.0045, \quad k = 0.0099. \end{aligned} \tag{A.12}$$

The pion energy distribution is then (here E_3 is the neutral pion energy)

$$\frac{d\Gamma}{dE_3} \propto \int ds_2 |\mathcal{A}|^2. \tag{A.13}$$

We then find that the energy distribution of π_0 in decays of $K_L \rightarrow \pi^+ \pi^- \pi^0$ at rest is proportional to

$$\begin{aligned} \frac{d\Gamma}{dE_3} &= \left[1 + g \frac{(s_3 - s_0)}{m_{\pi}^2} + h \left(\frac{s_3 - s_0}{m_{\pi}^2} \right)^2 \right. \\ &+ \left(j + f \frac{(s_3 - s_0)}{m_{\pi}^2} \right) \frac{(-3s_0 - s_3)}{m_{\pi}^2} \\ &+ \left. k \left(\frac{(-3s_0 - s_3)}{m_{\pi}^2} \right)^2 \right] \sigma \\ &+ \left(j + f \frac{(s_3 - s_0)}{m_{\pi}^2} + 2k \frac{(-3s_0 - s_3)}{m_{\pi}^2} \right) \\ &\times \sigma(3s_0 - s) + \frac{4}{3} k \frac{1}{m_{\pi}^4} \sigma \\ &\times \left(\frac{3}{4}(3s_0 - s)^2 + \frac{1}{4}\sigma^2 \right), \end{aligned} \tag{A.14}$$

where

$$\begin{aligned} \sigma &= \sqrt{1 - \frac{4M_{\pi}^2}{s} (s - (M_K + M_{\pi})^2)^{1/2}} \\ &\times (s - (M_K - M_{\pi})^2)^{1/2}. \end{aligned} \tag{A.15}$$

For the $K_L \rightarrow 3\pi^0$ decay, we have [15]

$$|\mathcal{A}|^2 = 1 + h \frac{(s_3 - s_0)^2}{m_+^4}, \tag{A.16}$$

where $h = 0.59$. The energy distribution may then be found similarly to the calculation for $K_L \rightarrow \pi^+ \pi^- \pi^0$ above.

Appendix A.4. $\omega \rightarrow \pi^0(p_1)\pi^+(p_2)\pi^-(p_3)$

ω decays to three pions are described by a similar Dalitz plot, which was taken from [30].

Appendix B. Boosting the decay spectrum

We now describe the general procedure to obtain the boosted spectrum from the decay spectrum at rest.

We consider a particle of mass m which decays into a number of daughter particles, and we assume that the kinematic distribution of the decay is known in the rest frame of the particle. Our goal is to determine the kinematic distribution in the lab frame, where the parent particle is moving. We take the parent particle to be travelling along the z -axis, with an energy E_m , corresponding to a Lorentz factor $\gamma = E_m/m$. We assume that there is no correlation between the direction of the daughter particle's momentum and the direction of the parent particle's boost.

In the CM frame, the four-momentum of one of the daughter particles is $(E', p' \sin \theta', 0, p' \cos \theta')$. We are given dP/dE' in the CM frame; i.e. the probability of obtaining in the CM frame a given value of the daughter particle's energy. In the lab frame, the four-momentum is $(E, p \sin \theta, 0, p \cos \theta)$. We are looking for dP/dE .

For the daughter particle in the lab frame, we have

$$E = \gamma(E' + p' \beta \cos \theta). \tag{B.1}$$

For any given E , this equation has a solution for $\cos \theta$ if E' lies in the range

$$\gamma(E - p\beta) \leq E' \leq \gamma(E + p\beta). \tag{B.2}$$

The kinematic distribution of the daughter particle in the laboratory frame is then

$$\begin{aligned} \frac{dP(E)}{dE} &= \frac{1}{2} \int dE' d \cos \theta \frac{dP(E')}{dE'} \delta \\ &\times (E - \gamma(E' + \beta p' \cos \theta)) \end{aligned}$$

$$= \frac{1}{2} \int_{E_1}^{E_2} dE' \frac{dP(E')}{dE'} \frac{1}{p'\beta\gamma}, \quad (\text{B.3})$$

where $E_2 = \gamma(E + p\beta)$ and $E_1 = \gamma(E - p\beta)$. This formula allows us to obtain the boosted spectrum from the decay spectrum at rest.

If we assume that the parent particle itself has a kinematic distribution in the laboratory frame given by dN_m/dE_m , we then find

$$\frac{dP(E)}{dE} = \frac{1}{2} \int dE_m \frac{dN_m}{dE_m} \int_{E_1(E_m)}^{E_2(E_m)} dE' \frac{dP(E')}{dE'} \frac{1}{p'\beta\gamma}. \quad (\text{B.4})$$

Moreover, if the daughter particle itself decays isotropically to some tertiary product, one can determine kinematic distribution of this tertiary product by simply repeating the above process, treating the daughter particle now as the parent to the tertiary particle.

We can apply this formalism to the case of π^0 , whose dominant decay is to two photons. In the rest frame, the photons have back-to-back momenta and the distribution is $dP/dE' = 2\delta(E' - \frac{m_\pi}{2})$, where the factor of two accounts for the two photons. We then find

$$\begin{aligned} \frac{dP}{dE} &= \int_{E\gamma(1-\beta)}^{E\gamma(1+\beta)} dE' \delta\left(E' - \frac{m_\pi}{2}\right) \frac{1}{E'\beta\gamma} \\ &= \frac{2}{\sqrt{E_\pi^2 - m_\pi^2}} \\ &\quad \times \left[\theta\left(E - \frac{m_\pi}{2} \sqrt{\frac{1-\beta}{1+\beta}}\right) \theta\left(\frac{m_\pi}{2} \sqrt{\frac{1+\beta}{1-\beta}} - E\right) \right]. \end{aligned} \quad (\text{B.5})$$

This reproduces the usual box distribution.

If the π^0 injection spectrum is given by dN_π/dE_π , then we may express the photon spectrum as [31]

$$\frac{dN_\gamma}{dE_\gamma} = \int_{\frac{m_\pi}{2} \left(\frac{2E_\gamma}{m_\pi} + \frac{m_\pi}{2E_\gamma}\right)}^{\infty} dE_\pi \left[\frac{dN_\pi}{dE_\pi} \frac{2}{\sqrt{E_\pi^2 - m_\pi^2}} \right]. \quad (\text{B.6})$$

This implies that the photon spectrum is log-symmetric about $m_\pi/2$ with a global maximum at that point. Moreover, the spectrum decreases monotonically as the energy either increases or decreases away from $m_\pi/2$. We see these features in figure 1.

The last thing which is needed is dN_π/dE_π . This can be determined from the procedure described above, treating π^0 as the daughter produced by the decay of K_L , K_S , K^\pm , ρ^\pm and ω . But there is one subtlety to note. This approach is strictly valid only if there is no correlation between the pion boost and the boost of the parent. This is necessarily true if the parent has spin-0, but need not be true if the parent is a vector meson. But

we shall assume that this effect is negligible, and ignore it henceforth.

References

- [1] e-ASTROGAM Collaboration: A De Angelis *et al*, [arXiv:1711.01265](https://arxiv.org/abs/1711.01265) [astro-ph.HE]
- [2] AMEGO Team: R Caputo *et al*, *PoS ICRC* **2017**, 910 (2017), <https://doi.org/10.22323/1.301.0910>
- [3] J H Buckley and APT Collaboration, The Advanced Pair Telescope (APT) Mission Concept, in *AAS/High Energy Astrophysics Division #10*, vol. 10, p. #37.04. Mar., 2008.
- [4] K K Boddy and J Kumar, *Phys. Rev. D* **92**(2), 023533 (2015), <https://doi.org/10.1103/PhysRevD.92.023533>, [arXiv:1504.04024](https://arxiv.org/abs/1504.04024) [astro-ph.CO]
- [5] K K Boddy and J Kumar, *AIP Conf. Proc.* **1743**, 020009 (2016), <https://doi.org/10.1063/1.4953276>, [arXiv:1509.03333](https://arxiv.org/abs/1509.03333) [astro-ph.CO]
- [6] K K Boddy, K R Dienes, D Kim, J Kumar, J C Park and B Thomas, *Phys. Rev. D* **94**(9), 095027 (2016), <https://doi.org/10.1103/PhysRevD.94.095027>, [arXiv:1606.07440](https://arxiv.org/abs/1606.07440) [hep-ph]
- [7] R Bartels, D Gaggero and C Weniger, *J. Cosmol. Astropart. Phys.* **1705**(05), 001 (2017), <https://doi.org/10.1088/1475-7516/2017/05/001>, 1703.02546 [astro-ph.HE]
- [8] O Cata, A Ibarra and S Inghenutt, *J. Cosmol. Astropart. Phys.* **1711**(11), 044 (2017), <https://doi.org/10.1088/1475-7516/2017/11/044>, 1707.08480 [hep-ph]
- [9] M Dutra, M Lindner, S Profumo, F S Queiroz, W Rodejohann and C Siqueira, *J. Cosmol. Astropart. Phys.* **1803**, 037 (2018), <https://doi.org/10.1088/1475-7516/2018/03/037>, [arXiv:1801.05447](https://arxiv.org/abs/1801.05447) [hep-ph]
- [10] J Kumar, [arXiv:1808.02579](https://arxiv.org/abs/1808.02579) [hep-ph]
- [11] D Choudhury and D Sachdeva, 1903.06049 [hep-ph]
- [12] C Terschlusen, S Leupold and M F M Lutz, *Eur. Phys. J. A* **48**, 190 (2012), <https://doi.org/10.1140/epja/i2012-12190-6>, [arXiv:1204.4125](https://arxiv.org/abs/1204.4125) [hep-ph]
- [13] J Gasser and H Leutwyler, *Nucl. Phys. B* **250**, 465 (1985)
J Gasser and H Leutwyler, *Ann. Phys.* **158**, 142 (1984)
U G Meissner, *Rep. Prog. Phys.* **56**, 903 (1993), hep-ph/9302247
G Ecker, *Prog. Part. Nucl. Phys.* **35**, 1 (1995), hep-ph/9501357
A Pich, *Rep. Prog. Phys.* **58**, 563 (1995), hep-ph/9502366
G Colangelo and G Isidori, hep-ph/0101264
S Scherer, *Adv. Nucl. Phys.* **27**, 277 (2003), hep-ph/0210398
- [14] C Terschlusen and S Leupold, *Phys. Rev. D* **94**(1), 014021 (2016), <https://doi.org/10.1103/PhysRevD.94.014021>, [arXiv:1603.05524](https://arxiv.org/abs/1603.05524) [hep-ph]
- [15] Particle Data Group: M Tanabashi *et al*, *Phys. Rev. D* **98**, 030001 (2018)

- [16] M Cirelli *et al*, *J. Cosmol. Astropart. Phys.* **1103**, 051 (2011), Erratum: *J. Cosmol. Astropart. Phys.* **1210**, E01 (2012), <https://doi.org/10.1088/1475-7516/2012/10/E01>, <https://doi.org/10.1088/1475-7516/2011/03/051>, arXiv:1012.4515 [hep-ph]
- [17] A Geringer-Sameth, S M Koushiappas and M Walker, *Astrophys. J.* **801**(2), 74 (2015), <https://doi.org/10.1088/0004-637X/801/2/74>, arXiv:1408.0002 [astro-ph.CO]
- [18] A W Strong, I V Moskalenko and O Reimer, *Astrophys. J.* **613**, 962 (2004), <https://doi.org/10.1086/423193> [astro-ph/0406254]
- [19] A Geringer-Sameth and S M Koushiappas, *Phys. Rev. Lett.* **107**, 241303 (2011), <https://doi.org/10.1103/PhysRevLett.107.241303>, arXiv:1108.2914 [astro-ph.CO]
- [20] M N Mazziotta, F Loparco, F de Palma and N Giglietto, *Astropart. Phys.* **37**, 26 (2012), <https://doi.org/10.1016/j.astropartphys.2012.07.005>, arXiv:1203.6731 [astro-ph.IM]
- [21] A Geringer-Sameth, S M Koushiappas and M G Walker, *Phys. Rev. D* **91**(8), 083535 (2015), <https://doi.org/10.1103/PhysRevD.91.083535>, arXiv:1410.2242 [astro-ph.CO]
- [22] K Boddy, J Kumar, D Marfatia and P Sandick, *Phys. Rev. D* **97**(9), 095031 (2018), <https://doi.org/10.1103/PhysRevD.97.095031>, arXiv:1802.03826 [hep-ph]
- [23] HAWC Collaboration: A Albert *et al*, *Astrophys. J.* **853**(2), 154 (2018), <https://doi.org/10.3847/1538-4357/aaa6d8>, arXiv:1706.01277 [astro-ph.HE]
- [24] T R Slatyer, *Phys. Rev. D* **87**(12), 123513 (2013), <https://doi.org/10.1103/PhysRevD.87.123513>, arXiv:1211.0283 [astro-ph.CO]
- [25] Planck Collaboration: N Aghanim *et al*, 1807.06209 [astro-ph.CO]
- [26] CRESST Collaboration: H Kluck *et al*, arXiv:1711.01285 [astro-ph.IM]
- [27] S Chang, J Liu, A Pierce, N Weiner and I Yavin, *J. Cosmol. Astropart. Phys.* **1008**, 018 (2010), <https://doi.org/10.1088/1475-7516/2010/08/018>, 1004.0697 [hep-ph]
- [28] J L Feng, J Kumar, D Marfatia and D Sanford, *Phys. Lett. B* **703**, 124 (2011), <https://doi.org/10.1016/j.physletb.2011.07.083>, arXiv:1102.4331 [hep-ph]
- [29] J L Feng, J Kumar and D Sanford, *Phys. Rev. D* **88**(1), 015021 (2013), <https://doi.org/10.1103/PhysRevD.88.015021>, arXiv:1306.2315 [hep-ph]
- [30] WASA-at-COSY Collaboration: P Adlarson *et al*, *Phys. Lett. B* **770**, 418 (2017), <https://doi.org/10.1016/j.physletb.2017.03.050>, arXiv:1610.02187 [nucl-ex]
- [31] K K Boddy, K R Dienes, D Kim, J Kumar, J C Park and B Thomas, *Phys. Rev. D* **95**(5), 055024 (2017), <https://doi.org/10.1103/PhysRevD.95.055024>, arXiv:1609.09104 [hep-ph]